Kimya / *Chemistry* **DOI: 10.21597/jist.687723**
Araştırma Makalesi / *Research Article*
Iğdır Üniversitesi Fen Bilimleri Enstitüsü Dergisi, 10(3): 1799-1810, 2020
Journal of the Institute of Science and Technology, 10(3): 1799-1810, 2020
ISSN: 2146-0574, eISSN: 2536-4618

Spectroscopic Comparison of 4-Isopropyl-N, N-Bis (4-Azidophenyl) Aniline molecule (IPAPA): DFT and MEP Analysis

Ertugrul CIFTCI[1], Ahmet Cagri ATA[1]*, Ümit YILDIKO[2], İsmail CAKMAK[1]

ABSTRACT: Nuclear magnetic resonance, vibrational, structural and electronic properties for 4-isopropyl-N, N-Bis (4-azidophenyl) aniline (IPAPA) were determined by quantum chemical calculations of the DFT method. The results were compared with experimental ^{1}H-NMR spectral data. Theoretical chemical calculations and experimental values were in harmony. The band gap of HOMO - LUMO indicates that the IPAPA molecule is chemically active and has charge transfer in the monomer. In addition, molecular electrostatic potential (MEPS) maps were drawn to identify the reactive regions of the IPAPA molecule. Hybrid functional B3LYP and hybrid exchange–correlation functional named CAM-B3LYP methods of density functional theory (DFT) were selected as the study method. In both methods, molecular optimization and electronic properties were obtained by using 6-311 ++ G (d, p) base set. In addition, HOMO and LUMO energies have been used to identify spherical reactivity and to determine chemical stability.

Keywords: Triphenyl Amine, DFT, HOMO-LUMO, MEPS.

4-İzopropil-N, N-Bis (4-Azidofenil) Anilin molekülünün (IPAPA) Spektroskopik Karşılaştırması: DFT ve MEP Analizi

ÖZET: 4-izopropil-N,N-Bis (4-Azidofenil) Anilin (IPAPA) için nükleer manyetik rezonans, titreşimsel, yapısal ve elektronik özellikler DFT yönteminin kuantum kimyasal hesaplamaları ile belirlenmiştir. Sonuçlar deneysel ^{1}H-NMR spektral verileri ile karşılaştırıldı. Teorik kimyasal hesaplamalar ve deneysel değerler uyum içindeydi. HOMO ve LUMO'nun bant boşluğu, IPAPA molekülünün kimyasal olarak aktif olduğunu ve monomerde yük transferine sahip olduğunu gösterir. Ek olarak, moleküler elektrostatik potansiyel (MEPS) haritaları IPAPA molekülünün reaktif bölgelerini tanımlamak için çizildi. Yoğunluk fonksiyonel teorisinin (DFT), CAM-B3LYP metotları olarak adlandırılan hibrid fonksiyonel B3LYP ve hibrid değişim-korelasyon fonksiyonu çalışma yöntemi olarak seçilmiştir. Her iki yöntemde de, moleküler optimizasyon ve elektronik özellikler 6-311 ++ G (d, p) baz seti kullanılarak elde edildi. Ek olarak, HOMO ve LUMO enerjileri küresel reaktiviteyi tanımlamak ve kimyasal kararlılığı belirlemek için kullanılmıştır.

Anahtar kelimeler: Trifenil Amin, DFT, HOMO-LUMO, MEPS.

[1]Ertuğrul CIFTCI (**Orcid ID:** 0000-0001-5866-8597), Ahmet Cagri ATA (**Orcid ID:** 0000-0002-2296-2265), İsmail CAKMAK (**Orcid ID:** 0000-0002-3191-7570), Kafkas Üniversitesi, Fen-Edebiyat Fakültesi, Kimya Bölümü, Kars, Türkiye
[2]Ümit YILDIKO (**Orcid ID:** 0000-0001-8627-9038), Kafkas Üniversitesi, Mühendislik-Mimarlık Fakültesi, Biyomühendislik Bölümü, Kars, Türkiye

*Sorumlu Yazar/Corresponding Author: Ahmet Çağrı ATA, e-mail: ahmetata1024@gmail.com

Geliş tarihi / *Received:* 11-02-2020
Kabul tarihi / *Accepted:* 28-04-2020

INTRODUCTION

Triphenylamine (TPA) derivatives have attracted great attention due to their electroactive properties and potential applications such as hall carriers, light emitters and photoconductors. TPA derivatives are electroactive conductive materials with an easily oxidizable electroactive core and excellent hall carrying capacity (Duan et al., 2019; Yadav et al., 2020). Therefore, the investigation of the electrochemical process of TPA based materials is a very important category. The triphenylamine derivatives, which are rich in electrons, are one of the promising donor parts of the donor-acceptor species of functional molecules because of their good electron-donating and high-hall carrier properties (Gu et al., 2009; Steponaitis et al., 2019). Triphenylamine derivatives are important molecules in numerous dye-sensitive solar cells due to the unique irregularity of the three phenyl substituents, the strong electronizing agent, the high light-to-electric conversion efficiency and good hall carrying capacity, and organic electroluminescence materials(Sęk et al., 2019; Yoosuf et al., 2019). Properties of triphenylamine-based derivatives were investigated using absorption, fluorescence spectroscopy, thermogravimetric analysis and density functional theory calculations (Bourass et al., 2019; Priyatha et al., 2019; Qian et al., 2017; Weng et al., 2016).

Nowadays, the theoretical calculation methods used are easily applied in the laboratory environment for non-synthesized or non-synthesized molecules and the desired results can be obtained. Computational chemistry is a branch of chemistry where computers are used as an aid in solving chemical problems (Boyd, 2019). In computational chemistry, effective computer programs are used to calculate structures, molecules and solid properties. Some theoretical computational studies provide more accurate results than experimental methods. The results of the studies performed by calculation methods are very reliable (Gu et al., 2009; Priyatha et al., 2019; Yadav et al., 2019).

In this study, 4-isopropyl-N, N-Bis (4-Azidophenyl) aniline (IPAPA) molecule synthesized by our group was first drawn with GaussView 6.0 and the input file was created. The ab-initio calculations were performed in Gaussian 09 package program. Hybrid functional B3LYP and hybrid exchange–correlation functional named CAM-B3LYP methods of density functional theory (DFT) were selected as the study method. In both methods, molecular optimization and electronic properties were obtained by using 6-311 ++ G (d, p) base set. The ^{1}H-NMR spectrum of the molecule was compared with theoretical calculations and experimental results.

MATERIALS AND METHODS

Theoretical analysis of ^{1}H-NMR spectra of some triphenyl amine derivative was performed by using Chem Office and Gaussian 09 programs (M. J. Frisch, 2016). IPAPA molecule was first drawn in the ChemBioDraw program for molecule for ab-initio calculations made in the Gaussian 09 program and minimized by the Chem3D program by SYBL2 (mol2). Minimized molecules were given to Gaussian 09 program and ab-initio calculations were made for the structure.

For molecule, the gas phase was first optimized using the base set of B3LYP 6-311G ++ G (d, p). Then, for molecule, both the gas phase CAM-B3LYP 6-311 G++ (d, p) optimization and freq calculation was performed. The ^{1}H-NMR spectra of the molecule were compared with the experimental results by theoretical calculations.

RESULTS AND DISCUSSION

Geometry Optimization

IPAPA optimized basic state structure and total energy conversion are given in Figure 1. DFT-B3LYP / CAM-B3LYP - 6-311 G++ (d, p) optimized bond lengths, bond angles and dihedral angles

parameters of the calculated molecule are listed in Tables 1 and 2. All the values calculated theoretically from the optimized geometry of IPAPA molecule were given and compared in Figure 2-3. This means that the structure has the minimum potential energy. All bond lengths and bond angles in the phenyl rings are within the normal range.

C-C bond distances of 1.08363-1.53993 Å for DFT and 1.08310 - 1.53209 Å for CAM-B3LYP, 1.41818-1.41983 Å for DFT and 1.41386 - 1.41855 Å for CAM-B3LYP belong to the nitrogen atom bound to the phenyl ring. The C-H lengths in the aromatic ring are 1.08322-1.09602 Å and the N-N length is 1.13465-1.23075 Å. All C-C-C angles range from 118 ° to 121 °. The C-C-H angle in the compound is 119 °-120 °, C-C-N 116 °-120 °, C-N-N 118 ° and N-N-N 172 °. There are very few differences between DFT and CAM-B3LYP values. Theoretically, calculated values of some triphenyl amine compounds can give an idea of the geometry of molecular changes.

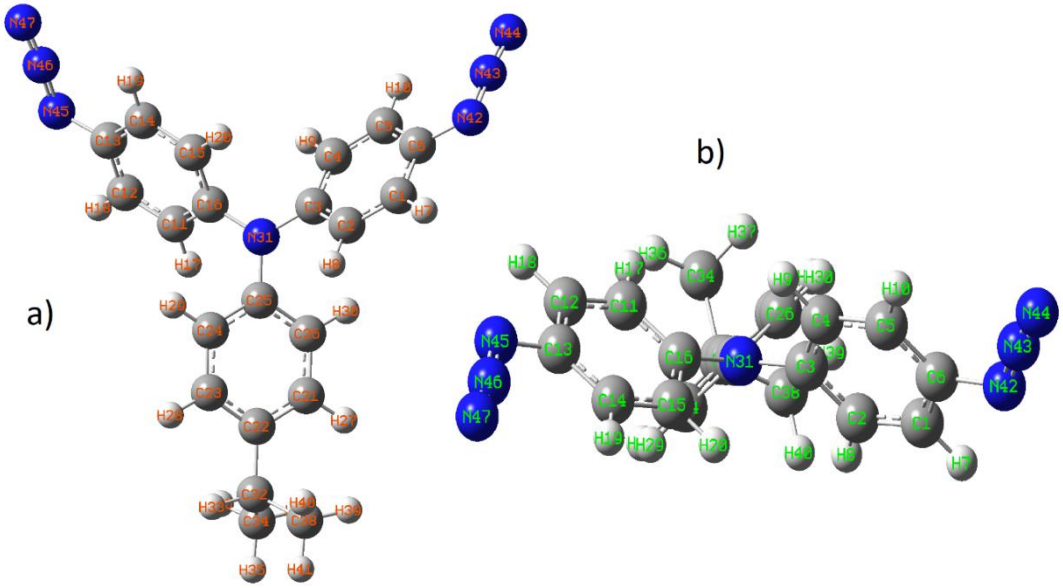

Figure 1. The three-dimensional atomic structure of IPAPA molecule is shown (a, b)

Table 1. Optimized geometrical parameters of IPAPA calculated at the B3LYP and CAM-B3LYP levels with 6–311++G(d,p) basis set

Bond Lengths (Å)	B3LPY	CAM-B3LYP	Bond Angles (º)	B3LPY	CAM-B3LYP
C1-C2	1.38735	1.38207	C1-C2-C3	120.83823	120.79397
C1-C6	1.39757	1.39065	C1-C6-C5	119.36696	119.44970
C1-H7	1.08322	1.08255	C1-C6-N42	116.50506	116.55052
C3-N31	1.41818	1.41386	C6-N42-N43	118.82183	117.74133
C6-N42	1.41977	1.41850	C2-C3-C4	118.40597	118.49869
C15-H20	1.08304	1.08251	C6-C1-H7	119.06626	118.99934
C14-H19	1.08460	1.08409	C6-C5-H10	120.54782	120.64902
N42-N43	1.23075	1.22677	N42-N43-N44	172.98864	173.90410
N43-N44	1.13465	1.12538	C1-C2-H8	119.63556	119.74498
C12-C13	1.39768	1.39078	N31-C3-C2	120.79322	120.71094
C12-H18	1.08323	1.08255	N31-C3-C4	120.80059	120.79019
C11-C12	1.38720	1.38192	C3-N31-C16	120.19963	120.21968
C13-N45	1.41983	1.41855	N31-C16-C15	120.82049	120.82449
N45-N46	1.23069	1.22673	C25-C26-H30	119.50876	119.46081
N46-N47	1.13468	1.12539	C11-C12-C13	120.33477	120.28904

Table 1. Optimized geometrical parameters of IPAPA calculated at the B3LYP and CAM-B3LYP levels with 6–311++G(d,p) basis set (continued)

C24-H29	1.08355	1.08302	C13-C14-H19	120.54168	120.64686
C23-C24	1.39254	1.38757	C12-C13-N45	116.50116	116.54348
C21-C22	1.40111	1.39466	C14-C13-N45	124.13911	124.00989
C22-C32	1.52136	1.51587	C13-N45-N46	118.82376	117.73957
C32-C34	1.53993	1.53209	C32-C34-H35	111.24436	110.65762
C32-H33	1.09602	1.09473	N45-N46-N47	172.99746	173.90600
C32-C38	1.53962	1.53184	C32-C34-H37	111.24436	111.12589
C34-H35	1.09413	1.09283	C26-C25-N31	120.64383	120.58889
C34-H36	1.09296	1.09177	C22-C32-C34	111.90613	111.75007
C34-H37	1.09413	1.09308	C32-C34-H36	111.23284	111.26713
C38-H39	1.09415	1.09308	C34-C32-C38	111.02104	110.94699
C38-H40	1.09298	1.09179	C32-C38-H39	111.31370	111.19158
C38-H41	1.09413	1.09283	C32-C38-H40	111.23292	111.26718
C26-C30	1.08363	1.08310	C32-C22-C21	121.77698	121.57295
C21-H27	1.08489	1.08429	C21-C26-H30	119.99943	120.08057
C23-H28	1.08563	1.08487	C25-N31-C16	119.92012	119.91356

Table 1 shows optimized bond angles and bond lengths of the compound selected on the basis of DFT and CAM-B3LYP / 6-311G++ (d, p). The difference is very small and shows a good fit between the two systems.

Table 2. Optimized geometrical parameters of IPAPA calculated at the B3LYP and CAM-B3LYP levels with 6–311++G(d,p) basis set

Dihedral Angles (º)	B3LPY	CAM-B3LYP	Dihedral Angles (º)	B3LPY	CAM-B3LYP
C1-C2-C3-C4	-0.19481	-0.28253	N42-C6-C1-H7	0.41423	0.35927
C1-C6-C5-C4	-0.30431	-0.38371	N45-C13-C12-H18	0.44360	0.37805
C1-C6-C5-H10	-179.34130	-179.46581	H7-C1-C2-H8	-0.29476	-0.26162
C1-C6-N42-N43	-179.65500	-179.85042	H9-C4-C5-H10	-0.12829	-0.11777
C2-C3-N31-C16	138.32142	138.57564	C24-C25-N31-C16	-43.64461	-43.29803
C6-C1-C2-H8	-179.36800	-179.38684	C22-C32-C34-H36	-56.29107	-56.38985
C6-N42-N43-N44	179.44234	179.75639	H33-C32-C34-H37	-179.30505	-179.32879
C11-C12-C13-N45	179.54793	179.52180	H27-C21-C22-C23	-179.45792	-179.53699
C11-C12-C13-C14	-0.47887	-0.48801	H35-C34-C32-H33	-59.69236	-59.77104
N31-C3-C4-H9	-0.40095	-0.29943	C22-C32-C38-H40	55.80680	56.02590
C12-C13-C14-H19	-179.36135	-179.48246	C22-C32-C34-H35	-176.51710	-176.72973
C13-N45-N46-N47	179.50126	179.75265	C22-C32-C34-H37	63.87021	63.71252

Table 2 shows optimized dihedral bond angles of the compound selected on the basis of DFT and CAM-B3LYP / 6-311G++ (d, p). The difference is very small and shows a good fit between the two systems.

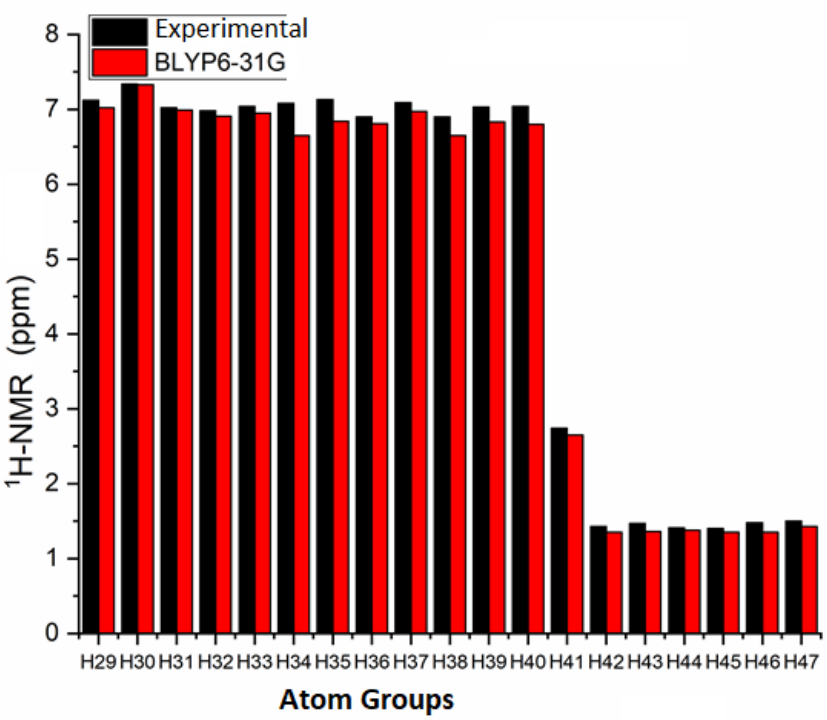

Figure 2. ^{1}H-NMR Experimental and Theoretical Chemical shift graph of IPAPA molecule

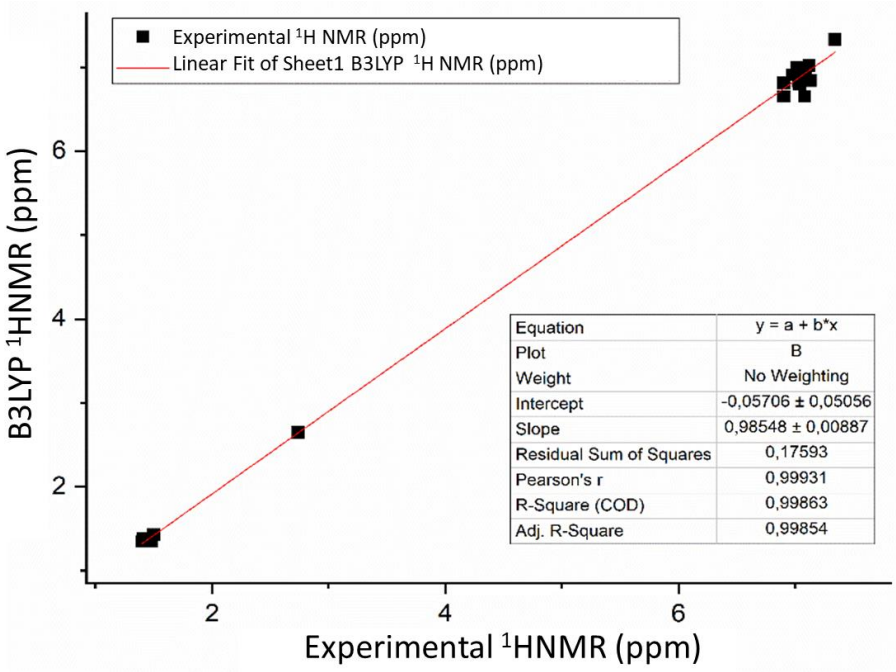

Figure 3. ^{1}H-NMR Experimental and Theoretical Calculations of IPAPA molecule are shown in the graph

Regression analysis was also performed for the compatibility of the experimental and theoretical data. In the regression analysis for the compatibility of both experimental and theoretical values, $experimental_{NMR}$ = a. $theoretical_{NMR}$ + b equation was used. According to this equation, whether two variables are compatible or not, a value should be close to or equal to 1 and b value should be close to or equal to 0.

HOMO and LUMO Analysis

HOMO shows a wide range of leading donor orbitals, while LUMO shows leading acceptor orbitals. The $HOMO_{-1}$ and $LUMO_{+1}$ orbitals represent the corresponding donor and acceptor levels with an energy state below and above these levels, respectively. HOMO are electrons in the outermost (highest energy) orbital that can function as an electron donor. LUMO is the innermost (lowest energy) orbital that has enough space to accept electrons and can act as an electron acceptor (Boxi et al., 2019; Damaceanu et al., 2018; Priyatha et al., 2019). Figures 4-5 are the density orbital representation of HOMO and LUMO for IPAPA. E_{LUMO+1} and E_{HOMO-1} graphs of the compound were also obtained. E_{LUMO} -1,4776 eV - E_{HOMO} -5,3300 eV for the B3LYP method and E_{LUMO} -0.2255 eV - E_{HOMO} -6,5376 eV for the CAM-B3LYP method were calculated from the figure. E_{LUMO+1} -1,3935 eV - E_{HOMO-1} -6,6647 eV for B3LYP method and E_{LUMO+1} -0.01959 eV - E_{HOMO-1} -8.0250 eV for CAM-B3LYP method were calculated. The calculated highest filled molecular orbital (HOMO) and lowest empty molecular orbital (LUMO) energies also confirm that charge transfer occurs within the molecule(Najare et al., 2019). The energy difference between the HOMO and LUMO energies, called the energy gap, helps the chemical reactivity and the kinetic stability of the molecule. Polarization shows the reactive indexes of a molecule with hardness, electronegativity and a small boundary orbital space. Table 3 shows the chemical reactivity indices.

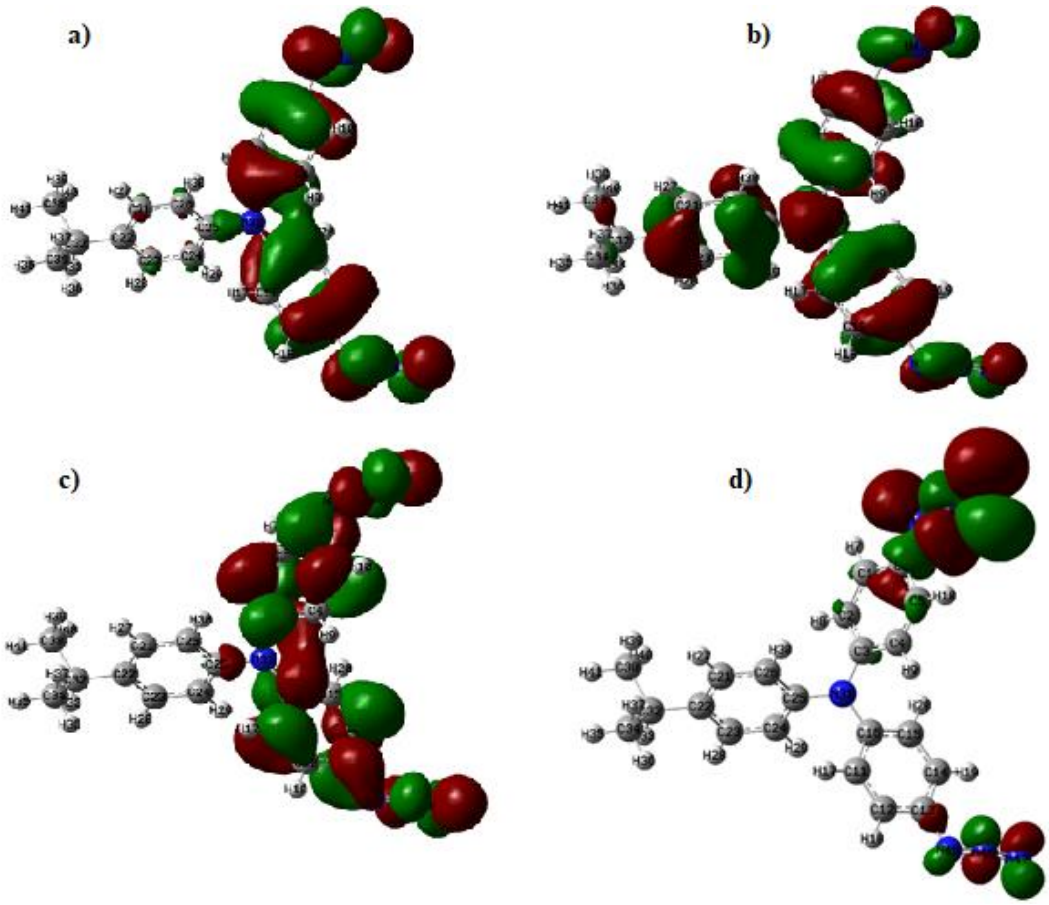

Figure 4. IPAPA molecule; **a) DFT_{HOMO-1}, b) DFT_{HOMO}, c) DFT_{LUMO}, d) DFT_{LUMO+1}** atomic orbital composition of a molecule

Table 3. Comparison of molecular properties of HOMO, LUMO, Energy gaps (HOMO – LUMO) and related IPAPA (au) using the DFT-CAM/B3LYP/6–311++G(d,p) method

Molecular Energy	**B3LYP**	**CAM-B3LYP**
E_{LUMO}	-1.4776	-0.2255
E_{HOMO}	-5.3300	-6.5376
Energy deficit (Δ)	-3.8524	-6.3121
Ionization Potential (I)	5.3300	6.5376
Electron Relevance (*A*)	1.4776	0.2255
Global Hardness (η)	-1.9262	-3.1560
Global Softness (*s*)	-0.9631	-1.5780
Chemical potential (μ)	3.4038	3.3815
Electronegativity (χ)	1.2388	0.6127
Global Electrophilicity (ω)	-6.0148	-1,1811

($A = -E_{LUMO}$, $= -E_{HOMO}$, $\eta = 1/2(E_{LUMO}-E_{HOMO})$, $\mu = 1/2(E_{HOMO}$ þ $E_{LUMO})$, $\omega = \mu^2/2\eta$, $S = 1/2\ \eta$, $\chi = (I + A)/2$, $\Delta = E_{LUMO} - E_{HOMO}$.)

Dipole moment is an important feature of the energy related to the electric field applied in the molecule. The dipole moment consists of intermolecular interactions involving the Van der Waals type dipole-dipole forces and generates strong intermolecular attraction. The dipole moment (μ) values of IPAPA molecule were calculated as 3.3628 Debye for B3LYP and 3.0239 Debye for CAM-B3LYP, respectively. Both methods show that the molecule has nonlinear properties.

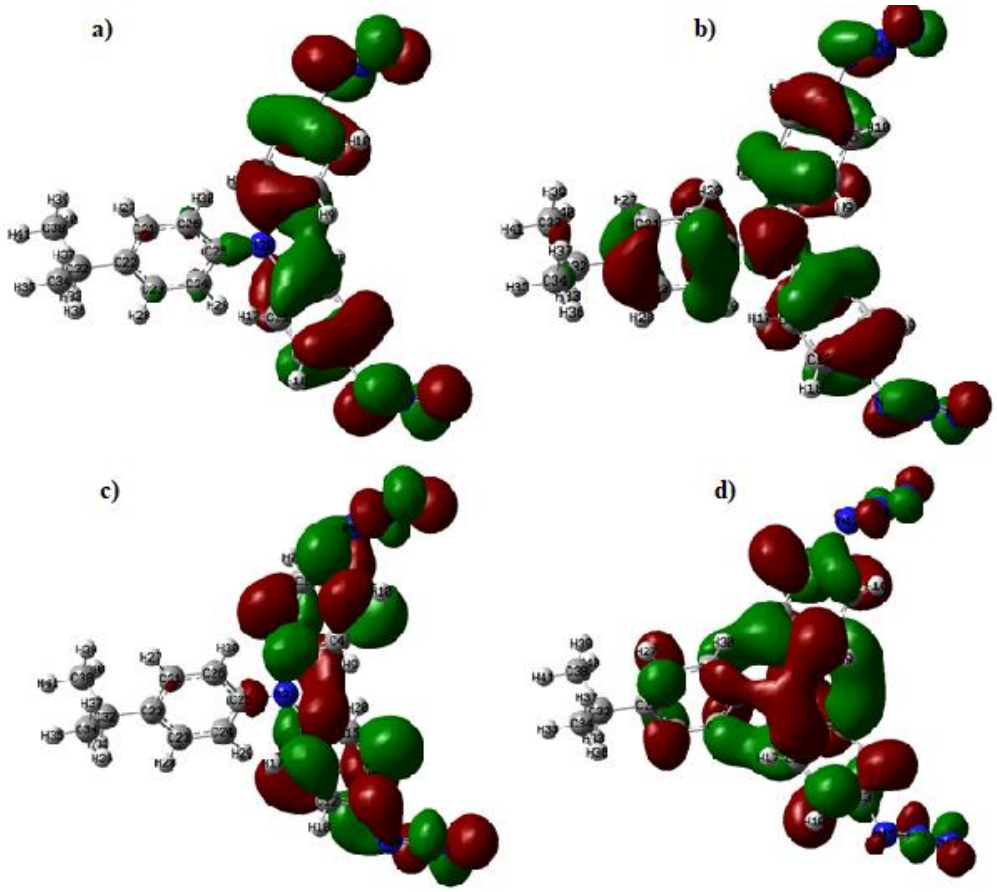

Figure 5. IPAPA molecule; **a) CAM$_{HOMO-1}$, b) CAM$_{HOMO}$, c) CAM$_{LUMO}$, d) CAM$_{LUMO+1}$** atomic orbital composition of a molecule

The parameters calculated in Table 5 show the electronic dipole moment and the total dipole moment. It can be calculated using the following equation.

$< \alpha > = 1/3\ (\alpha_{xx} + \alpha_{yy} + \alpha_{zz})$

$< \beta_{tot} > = [\ (\beta_{xxx} + \beta_{xyy} + \beta_{xzz})^2 + (\beta_{yyy} + \beta_{yzz} + \beta_{yxx})^2 + (\beta_{zzz} + \beta_{zxx} + \beta_{zyy})^2\ ]^{1/2}$

Table 4. Basic set of CAM with DFT B3LYP / 6-311G++ (d, p), calculated dipole moments of electricity (Debye), (au) polarisability, β components and β tot 4-isopropyl-N, N-Bis (4- Azidophenyl) Aniline value

Parameters	B3LYP	CAM-B3LYP	Parameters	B3LYP	CAM-B3LYP	Parameters	B3LYP	CAM-B3LYP
μ_x	-3.3384	-2.9997	α_{xx}	-168.4820	-166.7202	β_{XXX}	-129.0892	-116.8850
μ_y	-0.3968	-0.3744	α_{yy}	-184.6869	-183.1794	β_{XXY}	9.8159	8.0053
μ_z	-0.0794	-0.0742	α_{zz}	-163.3488	-163.6825	β_{XYY}	-110.2374	96.6208
$\mu_{(D)}$	3.3628	3.0239	α_{XY}	2.4855	2.5158	β_{YYY}	-37.5913	-34.0256
			α_{XZ}	0.4174	0.3699	β_{XXZ}	0.1053	-0.3011
			α_{YZ}	-1.1425	-0.3026	β_{XYZ}	-21.4529	-18.6032
			α (au)	-172,1725	-171,1940	β_{YYZ}	-5.8448	-5.0772
						β_{XZZ}	0.7633	0.2473
						β_{YZZ}	-0.2082	-0.3079
						β_{ZZZ}	1.0690	-1.1016
						β (esu)	$2.4x10^{-32}$	$3.3x10^{-32}$

Molecular Electrostatic Potential Surface (MEPS)

The molecular electrostatic potential surface (MEPS) are useful amounts to show charge distributions of molecules and visualize variable charged molecule regions and is plotted for the IPAPA molecule. Molecular electrostatic potential (MEPS) mapping plays an important role in investigating many features of the molecular structure. MEPS is widely used as a reactivity map to understand the hydrogen bonding interactions on organic molecules as well as electrophilic and nucleophilic reactions. Some of the molecule with negative electrostatic potential is sensitive to electrophilic attacks (Dwivedi et al., 2015; Srivastava et al., 2015).Different values of the electrostatic potential on the surface are shown in different colors (blue to red). The strongest attraction is represented by the positive (blue color) region, while the strongest repulsion is represented by the negative (red color) region. The green color indicates neutral electrostatic potential (Jayashree et al., 2019). Negative (red, orange and yellow) regions of MEPS show electrophilic reactivity and positive (blue color) ones belong to the nucleophilic reactivity region.

In this study, molecular electrostatic potential (MEPS) was coupled with 4 IPAPA maps as shown in Figure 6-7. In the case of IPAPA molecule, there are negative regions of the nitrogen atoms characterized by red in the MEPS map. IPAPA relatively large region around the nitrogen atoms of the aniline molecule represents the most negative potential region (dark red) and is suitable for electrophilic interaction. The hydrogen atom carries the maximum strength of the positive charge (dark blue). The aromatic ring region shows an almost neutral potential, most of which is represented by green colors.

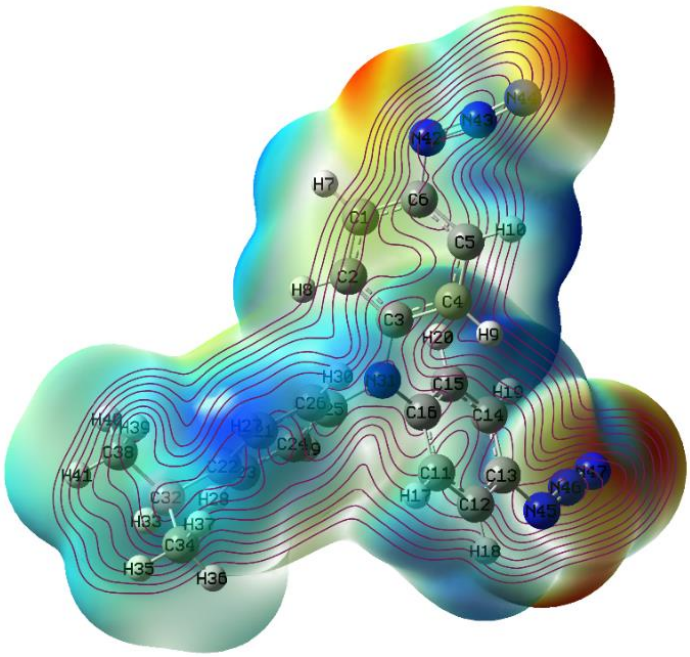

Figure 6. Molecular electrostatic potential of IPAPA

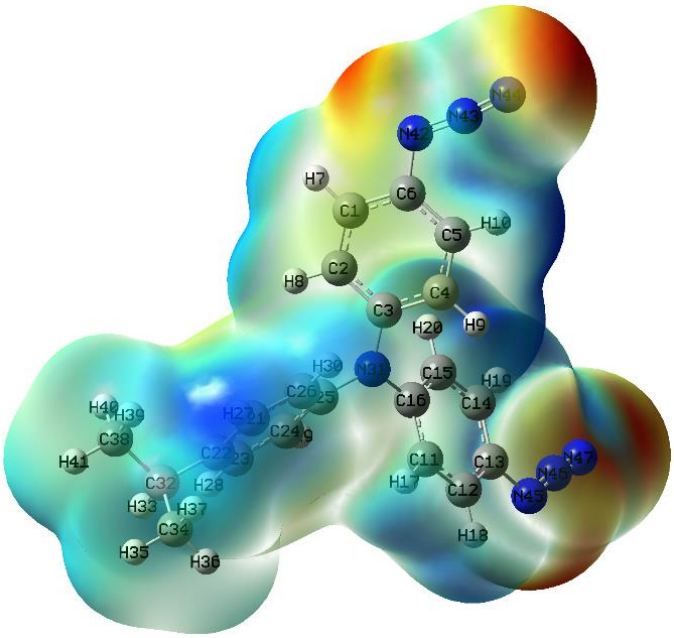

Figure 7. Molecular electrostatic potential of IPAPA

Mulliken Atomic Charges

The atomic charges play an important role in the application of quantum chemical calculations of molecular system because of the atomic charges affect dipole moment, polarizability, electronic structure, vibrational spectra and more properties for a molecular system (Téllez Soto et al., 2013). The charge distribution in the atom indicates the formation of donor and acceptor pairs, including charge transfer within the molecule (Priya et al., 2019). Mulliken atom was calculated using the DFT and CAM methods in the base set B3LYP / 6-311G++ (d, p). The data obtained are presented in Figure 8-9 and Table 5. The distribution of the mullikene charge of the nitrogen atom N attached to the aromatic ring is N31 (0.852537) - (0.793107), N42 (0.355902) - (-0.033063), N43 (0.046818) - (-0.029280), N44 (-0.258854) - (-) 0.278103), N45 (0.363991) - (0.448551), N46 (0.049169) - (-0.033063), and N47 (-

0.270415) - (-0.283405) indicate a negative charge. The charge value of the H atom attached to the aromatic ring has a positive charge. Some C atoms were observed to be positive and others negative.

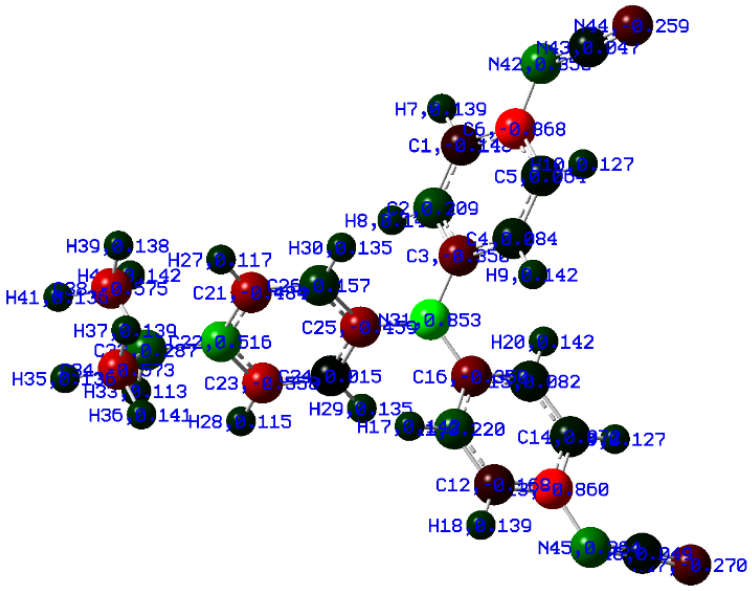

Figure 8. Mulliken atomic charges of IPAPA

Table 5. Mulliken atomic charges were calculated with B3LYP and CAM B3LYP / 6-311G++ (d,p)

	B3LYP	CAM-B3LYP		B3LYP	CAM-B3LYP
C1	-0.147582	-0.012631	N43	0.046818	-0.029280
C2	0.209087	0.079071	N44	-0.258854	-0.278103
C3	0.349759	-0.244121	N45	0.363991	0.448551
C4	0.083747	0.037754	N46	0.049169	-0.033063
C5	0.064443	0.055930	H7	0.138957	0.149517
C6	-0.868131	-0.876341	H8	0.142649	0.154376
C11	0.219670	0.124314	H9	0.141830	0.152190
C12	-0.168464	-0.047091	H10	0.127499	0.134440
C13	-0.860012	-0.889883	H17	0.142492	0.154072
C14	0.072342	0.058752	H18	0.138727	0.149690
C15	0.081539	0.033483	H19	0.127460	0.134389
C16	-0.350165	-0.262252	H20	0.142480	0.152670
C21	-0.483687	-0.277844	H27	0.117111	0.126677
C22	0.516294	0.318152	H28	0.115338	0.124321
C23	-0.558061	-0.353494	H29	0.134860	0.145142
C24	0.014625	-0.111687	H30	0.134574	0.144710
C25	-0.458647	-0.381255	H33	0.112695	0.120309
C26	0.157161	-0.070516	H35	0.135756	0.138059
C32	0.286690	0.187423	H36	0.140764	0.143610
C34	-0.572865	-0.557127	H37	0.138521	0.140009
C38	-0.575038	-0.553779	H39	0.138056	0.139249
N31	0.852537	0.793107	H40	0.142051	0.144579
N42	0.355902	0.439243	H41	0.135844	0.138082

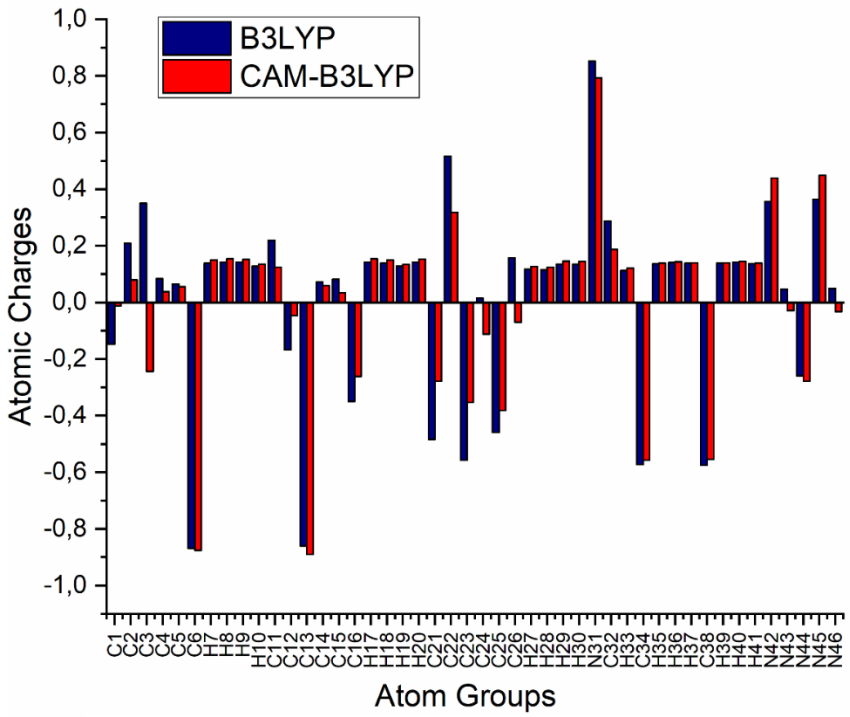

Figure 9. Comparison of IPAPA Mulliken atomic charges by two methods

CONCLUSION

In general, good agreement was obtained between experimental results synthesized in laboratory and theoretical results. In this case, it showed the reliability of the theoretical method used and good results were obtained with 6-31G ++ (d,p) basic set of B3LYP/CAM-B3LYP method for the theoretical calculation of IPAPA. Molecules were drawn in the ChemBioDraw program and transferred to Gaussian 09 program and the proton NMR data were very close to the experimental data. Thus, by considering these data for future studies, it will provide important facilities for the synthesis of molecules by minimizing the chemical consumption of the molecules to be synthesized in the future and making necessary predictions. As a result, the synthesized IPAPA were characterized by various theoretical methods and their structures were determined.

REFERENCES

Bourass M, El Alamy, A, & Bouachrine, M. (2019). Structural and photophysical studies of triphenylamine-based nonlinear optical dyes: effects of π-linker moieties on the D-π-A structure. Comptes Rendus Chimie, 22(5), 373-385.

Boxi S, Jana, D, & Ghorai, BK. (2019). Synthesis and optical properties of bipolar quinoxaline-triphenylamine based stilbene compounds. Optical Materials: X, 1, 100013.

Boyd RJ. (2019). Theoretical and Computational Chemistry. In Reference Module in Chemistry, Molecular Sciences and Chemical Engineering: Elsevier.

Damaceanu M-D, Constantin, C-P, Bruma, M, & Begunov, RS. (2018). The photo-optical and electrochemical activity promoted by trifluoromethyl-substituted and ortho-catenated triphenylamine core in poly(ether-imide)s. Polymer, 151, 34-46.

Duan L, Chen, Y, Zong, X, Liu, R, Sun, Z, Liang, M, Wu, Q, & Xue, S. (2019). Facile synthesis of triphenylamine-based hole-transporting materials for planar perovskite solar cells. Journal of Power Sources, 435, 226767.

Dwivedi A, Srivastava, AK, & Bajpai, A. (2015). Vibrational spectra, HOMO, LUMO, MESP surfaces and reactivity descriptors of amylamine and its isomers: A DFT study. Spectrochimica Acta Part A: Molecular and Biomolecular Spectroscopy, 149, 343-351.

Gu D, Yang, G, He, Y, Qi, B, Wang, G, & Su, Z. (2009). Triphenylamine-based pH chemosensor: Synthesis, crystal structure, photophysical properties and computational studies. Synthetic Metals, 159(23), 2497-2501.

Jayashree A, Narayana, B, Kumar, SM, Raghi, KR, Sarojini, BK, & Kumar, TKM. (2019). Synthesis, X-ray crystal structure, Hirshfeld surface analysis, DFT, MESP and molecular docking studies of 2-(4-bromophenyl)-1-(3-fluoro-4-methylphenyl)-4,5-diphenyl-1H-imidazole. Chemical Data Collections, 21, 100237.

M. J. Frisch GWT, H. B. Schlegel, G. E. Scuseria, M. A. Robb, J. R. Cheeseman, G. Scalmani, V. Barone, G. A. Petersson, H. Nakatsuji, X. Li, M. Caricato, A. Marenich, J. Bloino, B. G. Janesko, R. Gomperts, B. Mennucci, H. P. Hratchian, J. V. Ortiz, A. F. Izmaylov, J. L. Sonnenberg, D. Williams-Young, F. Ding, F. Lipparini, F. Egidi, J. Goings, B. Peng, A. Petrone, T. Henderson, D. Ranasinghe, V. G. Zakrzewski, J. Gao, N. Rega, G. Zheng, W. Liang, M. Hada, M. Ehara, K. Toyota, R. Fukuda, J. Hasegawa, M. Ishida, T. Nakajima, Y. Honda, O. Kitao, H. Nakai, T. Vreven, K. Throssell, J. A. Montgomery, Jr., J. E. Peralta, F. Ogliaro, M. Bearpark, J. J. Heyd, E. Brothers, K. N. Kudin, V. N. Staroverov, T. Keith, R. Kobayashi, J. Normand, K. Raghavachari, A. Rendell, J. C. Burant, S. S. Iyengar, J. Tomasi, M. Cossi, J. M. Millam, M. Klene, C. Adamo, R. Cammi, J. W. Ochterski, R. L. Martin, K. Morokuma, O. Farkas, J. B. Foresman, and D. J. Fox. (2016). Gaussian 09, Revision A.02, Gaussian, Inc., Wallingford CT,.

Najare MS, Patil, MK, Nadaf, AA, Mantur, S, Inamdar, SR, & Khazi, IAM. (2019). Synthesis, characterization and photophysical properties of a new class of pyrene substituted 1,3,4-oxadiazole derivatives. Optical Materials, 88, 256-265.

Priya MK, Revathi, BK, Renuka, V, Sathya, S, & Asirvatham, PS. (2019). Molecular Structure, Spectroscopic (FT-IR, FT-Raman, 13C and 1H NMR) Analysis, HOMO-LUMO Energies, Mulliken, MEP and Thermal Properties of New Chalcone Derivative by DFT Calculation. Materials Today: Proceedings, 8, 37-46.

Priyatha E, Sathishkumar, C, Palanisami, N, Venkatachalam, S, & Venkateswaran, R. (2019). Conjugated hole-transport molecules based on triphenylamine and aminoflourene: Synthesis, structural, solvatochromic and electrochemical properties. Journal of Molecular Structure, 1179, 145-153.

Qian X, Lan, X, Yan, R, He, Y, Huang, J, & Hou, L. (2017). T-shaped (D)2–A–π–A type sensitizers incorporating indoloquinoxaline and triphenylamine for organic dye-sensitized solar cells. Electrochimica Acta, 232, 377-386.

Sęk D, Kotowicz, S, Kula, S, Siwy, M, Szłapa-Kula, A, Małecki, JG, Maćkowski, S, & Schab-Balcerzak, E. (2019). Thermal, spectroscopic, electrochemical, and electroluminescent characterization of malononitrile derivatives with triphenylamine structure. Spectrochimica Acta Part A: Molecular and Biomolecular Spectroscopy, 210, 136-147.

Srivastava AK, Pandey, AK, Jain, S, & Misra, N. (2015). FT-IR spectroscopy, intra-molecular C−H···O interactions, HOMO, LUMO, MESP analysis and biological activity of two natural products, triclisine and rufescine: DFT and QTAIM approaches. Spectrochimica Acta Part A: Molecular and Biomolecular Spectroscopy, 136, 682-689.

Steponaitis M, Komskis, R, Kamarauskas, E, Malinauskas, T, Jursenas, S, & Getautis, V. (2019). Investigation of photophysical properties of triphenylamine phenylethenyl derivatives containing tertiary amine groups. Dyes and Pigments, 166, 122-129.

Téllez Soto CA, Costa, AC, Ramos, JM, Vieira, LS, Rost, NCV, Versiane, O, Rangel, JL, Mondragón, MA, Raniero, L, & Martin, AA. (2013). Surface enhanced Raman scattering, electronic spectrum, natural bond orbital, and mulliken charge distribution in the normal modes of diethyldithiocarbamate copper (II) complex, [Cu(DDTC)2]. Spectrochimica Acta Part A: Molecular and Biomolecular Spectroscopy, 116, 546-555.

Weng D, Shi, Y, Zheng, J, & Xu, C. (2016). High performance black-to-transmissive electrochromic device with panchromatic absorption based on TiO2-supported viologen and triphenylamine derivatives. Organic Electronics, 34, 139-145.

Yadav SB, Kothavale, S, & Sekar, N. (2019). Triphenylamine and N-phenyl carbazole-based coumarin derivatives: Synthesis, solvatochromism, acidochromism, linear and nonlinear optical properties. Journal of Photochemistry and Photobiology A: Chemistry, 382, 111937.

Yadav SB, Sonvane, SS, & Sekar, N. (2020). Novel blue-green emitting NLOphoric triphenylamine-imidazole based donor-π-acceptor compound: Solvatochromism, DFT, TD-DFT and non-linear optical studies. Spectrochimica Acta Part A: Molecular and Biomolecular Spectroscopy, 224, 117421.

Yoosuf M, Pradhan, SC, Soman, S, & Gopidas, KR. (2019). Triple bond rigidified anthracene-triphenylamine sensitizers for dye-sensitized solar cells. Solar Energy, 188, 55-65.